Competing field pulse induced dynamic transition in Ising models

Arnab Chatterjee* and Bikas K Chakrabarti†
Saha Institute of Nuclear Physics
1/AF Bidhannagar, Kolkata 700 064, India.

The dynamic magnetization-reversal phenomena in the Ising model under a finite-duration external magnetic field competing with the existing order for $T < T_c^0$ has been discussed. The nature of the phase boundary has been estimated from the mean-field equation of motion. The susceptibility and relaxation time diverge at the MF phase boundary. A Monte Carlo study also shows divergence of relaxation time around the phase boundary. Fluctuation of order parameter also diverge near the phase boundary. The behavior of the fourth order cumulant shows two distinct behavior: for low temperature and pulse duration region of the phase boundary the value of the cumulant at the crossing point for different system sizes is much less than that corersponding to the static transition in the same dimension which indicate a new universality class for the dynamic transition. Also, for higher temperature and pulse duration, the transition seem to fall in a mean-field like weak-singularity universality class.

PACS numbers: 05.50.+q; 05.70.Fh

I. INTRODUCTION

Thin films of ferromagnetic materials are of considerable interest as potential materials for the use as ultra-high density recording medium. Recently, sophisticated experimental techniques such as the magnetic force microscopy have enabled physicists to look at the magnetization state and switching mechanism of ferromagnetic particles in the nanometre scale [1]. Experiments [2, 3] on iron sesquilayers grown on tungsten are interesting from the theoretical point of view as the results seem to correspond precisely to an ideal ferromagnetic Ising system [3].

The response of a pure magnetic system to time-dependent external magnetic fields has been of current interest in statistical physics [4, 5, 6, 7]. These studies, having close applications in recording and switching industry, have also got considerable scientific and technical interest. These spin systems, driven by time-dependent external magnetic fields, have basically got a competition between two time scales: the time-period of the driving field and the relaxation time of the driven system. This gives rise to interesting non-equilibrium phenomena. Tóme and Oliveira first made a mean-field study [8] of kinetic Ising systems under oscillating field. The existence of the dynamic phase transition for such a system and its nature have been thoroughly studied using extensive Monte-Carlo simulations [5, 9]. Recently, Junier and Kurchan [10] have shown that the dynamics under oscillating field can induce asymmetry in the order parameter; namely an isotropic Heisenberg model (classical) under an alternating field switches to XY-like or Ising-like behavior, as the external field frequency and amplitude is tuned.

Later, investigations were extended to the dynamic response of (ferromagnetic) pure Ising systems under magnetic fields of finite-time duration [11, 12]. All the studies with pulsed field were made below T_c^0, the static critical temperature (without any field), where the system gets ordered. A 'positive' pulse is one which is applied along the direction of prevalent order, while the 'negative' one is applied opposite to that. The results for the positive pulse case did not involve any new thermodynamic scale [11]. In the negative pulse case, however, interesting features were observed [7, 12, 13, 14, 15, 16]: the negative field pulse competes with the existing order, and the system makes a transition from one ordered state characterised by an equilibrium magnetisation $+m_0$ (say) to the other equivalent ordered state with equilibrium magnetisation $-m_0$, depending on the temperature T, field strength h_p and its duration Δt. This transition is well studied in the limit $\Delta t \to \infty$ for any non-zero value of h_p at any $T < T_c^0$. This transition, for the general cases of finite Δt, is called here 'magnetisation-reversal' transition. As in the oscillating field case, in the study of magnetizatin-reversal transition, the finite duration (Δt) of the external field introduces a competition between two time scales: the relaxation time of the system and Δt. Some aspects of this transition has recently been studied extensively [6, 7, 12, 13, 14]. Recently, studies on switching behavior of some thin films of 'perpendicular media' (where spins are Heisenberg like rather than Ising like) have identified the same transition and

*Electronic address: arnab@cmp.saha.ernet.in
†Electronic address: bikas@cmp.saha.ernet.in

its phase boundary has been obtained both experimentally and theoretically [17].

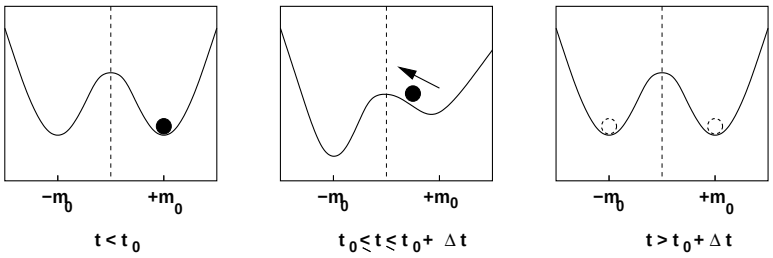

FIG. 1. Schematic diagram showing the free energy landscape against the magnetization at different times. For $t < t_0$ the landscape is symmetric with respect to $m = 0$ and the system is in $+m_0$ state as shown by • . For $t_0 \leq t \leq t_0 + \Delta t$, the landscape acquires a global minimum at $m = -m_0$ due to the presence of the external field and the system starts moving towards it. Beyond $t = t_0 + \Delta t$, the landscape again becomes symmetric and the system eventually stabilizes in either of the equivalent minima as shown by ∘.

II. MODEL AND THE TRANSITION

The model studied here is the Ising model with nearest-neighbour interaction under a time-dependent external magnetic field. This is described by the Hamiltonian:

$$H = -\sum_{\{ij\}} J_{ij} S_i S_j - h(t) \sum_i S_i, \tag{1}$$

where J_{ij} is the cooperative interaction between the spins at site i and j respectively, and each nearest-neighbour pair is denoted by $\{...\}$. We consider a square lattice. The static critical temperature is $T_c^0 = 2/\ln(1+\sqrt{2}) \simeq 2.269...$ (in units of J/K_B). At $T < T_c^0$, an external field pulse is applied, after the system is brought to equilibrium characterised by an equilibrium magnetisation $m_0(T)$. The spatially uniform field has a time-dependence as follows:

$$h(t) = \begin{cases} -h_p & t_0 \leq t \leq t_0 + \Delta t \\ 0 & \text{otherwise.} \end{cases} \tag{2}$$

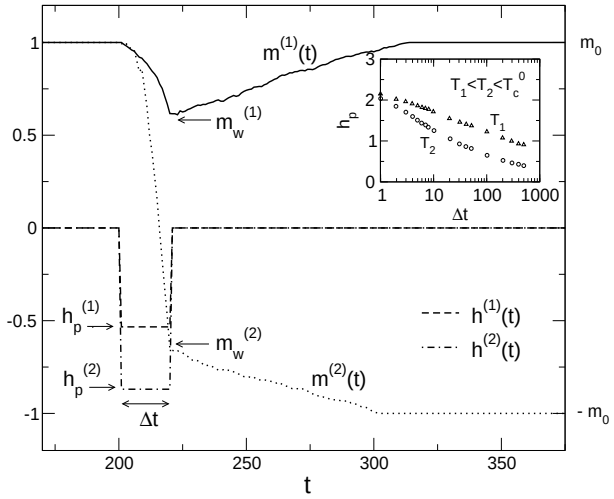

FIG. 2. Typical time variation of the response magnetisation $m(t)$ for two different field pulses $h(t)$ with same Δt for an Ising system at a fixed temperature T. The magnetisation-reversal here occurs due to increased pulse strength, keeping their width Δt same. The transition can also be brought about by increasing Δt, keeping h_p fixed. The inset indicates the typical phase boundaries (where the field withdrawal-time magnetisation $m_w = 0$) for two different temperatures (sequential updating; note that for random updating the phase boundaries shift upwards).

Typical time-dependent (response) magnetisation $m(t)$ ($= < S_i >$, where $< \ldots >$ denotes the thermodynamic 'ensemble' average) of the system under different magnetic field $h(t)$ are indicated in the Fig. 2. The time t_0 at which the pulse is applied is chosen such that the system reaches its equilibrium at T ($< T_c^0$). As soon as the field is applied, the magnetisation $m(t)$ starts decreasing, continues until time $t + \Delta t$ when the field is withdrawn. The system relaxes eventually to one of the two equlibrium states (with magnetisation $-m_0$ or $+m_0$). At a particular temperature T, for appropriate combinations of h_p and Δt, a magnetisation-reversal transition occurs, when the magnetisation of the system switches from one state of equilibrium magnetisation m_0 to the other with magnetisation $-m_0$. This reversal phenomena at $T < T_c^0$ is simple and well studied for $\Delta t \to \infty$ for any non-zero h_p. We study here the dynamics for finite Δt values. It appears that generally $h_p \to \infty$ as $\Delta t \to 0$ and $h_p \to 0$ as $\Delta t \to \infty$ for any such dynamic magnetisation-reversal transition phase boundary at any temperature T ($< T_c^0$). In fact, a simple application of the domain nucleation theory gives $h_p \ln \Delta t$ = constant along the phase boundary, where the constant changes by a factor $1/(d+1)$, where d denotes the lattice dimension, as the boundary changes from single to multi-domain region [11].

III. MEAN-FIELD STUDY

Consider a system of N Ising spins in contact with a heat bath evolving under Glauber single spin flip dynamics. The master equation can be written as [18]

$$\frac{d}{dt}P\left(S_1, \cdots, S_N; t\right) \;=\; -\sum_j W_j(S_j) P\left(S_1, \ldots, S_N; t\right) + \sum_j W_j(-S_j) P\left(S_1, \ldots, -S_j, \ldots, S_N; t\right),$$

where $P\left(S_1, \cdots, S_N; t\right)$ is the probability to find the spins in the configuration $(S_1, \cdots, S_N)$ at time t and $W_j(S_j)$ is the probability of flipping of the jth spin. Satisfying the condition of detailed balance one can write the transition probability as

$$W_j(S_j) = \tfrac{1}{2\lambda}\left[1 - S_j \tanh\left(\tfrac{\sum_i J_{ij} S_i(t) + h_j}{T}\right)\right],$$

where λ is a temperature dependent constant. Defining the spin expectation value as

$$m_i = \langle S_i \rangle = \textstyle\sum_S S_i P\left(S_1, \ldots, S_N; t\right),$$

where the summation is carried over all possible spin configurations, one can write

$$\lambda \frac{dm_i}{dt} = -m_i + \left\langle \tanh\left(\frac{\sum_j J_{ij} S_j + h_i}{T}\right)\right\rangle. \tag{3}$$

Using the mean field approximation linearisation (in m), (3) can be written after a Fourier transform,

$$\frac{dm_q(t)}{dt} = \lambda^{-1}\left[\left(K(q) - 1\right) m_q(t) + \frac{h_q(t)}{T}\right], \tag{4}$$

where $K(q) = J(q)/T$. When we are concerned only with the homogeneous magnetization, we consider the $q = 0$ mode of the equation and writing $m_{q=0} = m$ and $h_{q=0} = h$, we get

$$\frac{dm}{dt} = \lambda^{-1}\left[\left(K(0) - 1\right) m(t) + \frac{h(t)}{T}\right]. \tag{5}$$

In the mean field approximation $K(0) = T_c^{MF}/T$ with $T_c^{MF} = J(0)$ and for small q, $K(q) \simeq K(0)\left(1 - q^2\right)$. Differentiating (4) with respect to the external field, we get the rate equation for the dynamic susceptibility $\chi_q(t)$ as

$$\frac{d\chi_q(t)}{dt} = \lambda^{-1}\left[\left(K(q) - 1\right) \chi_q(t) + \frac{1}{T}\right]. \tag{6}$$

We divide the entire time zone in three different regimes : (I) $0 < t < t_0$, where $h(t) = 0$ (II) $t_0 \leq t \leq t_0 + \Delta t$, where $h(t) = -h_p$ and (III) $t_0 + \Delta t < t < \infty$, where $h(t) = 0$ again. We note that (5) can be readily solved separately for the three regions as the boundary conditions are exactly known. In region I, $dm/dt = 0$ and the solution of the linearized (5) becomes trivial. We, therefore, use the solution of (4) in region I ($m_0 = \tanh\left(m_0 T_c^{MF}/T\right)$) as the initial value of m for region II. Integrating (5) in region II, we then get

$$m(t) = \frac{h_p}{\Delta T} + \left(m_0 - \frac{h_p}{\Delta T}\right) \exp\left[b\Delta T\,(t - t_0)\right], \tag{7}$$

where $b = 1/\lambda T$ and $\Delta T = T_c^{MF} - T$. We also note that in order to justify the validity of the linearization of (4) one must keep the factor inside the exponential of (7) small. This restricts the linear theory to be valid close to T_c^{MF} and for small Δt. Writing $m_w \equiv m(t_0 + \Delta t)$, we get from (7)

$$m_w = \frac{h_p}{\Delta T} + \left(m_0 - \frac{h_p}{\Delta T}\right) e^{b\Delta T \Delta t}. \tag{8}$$

It is to be noted here that in absence of fluctuations, the sign of $m_w(h_p, \Delta t)$ solely decides which of the final two equilibrium states will be chosen by the system after the withdrawal of the pulse. At $t = t_0 + \Delta t$, if $m_w > 0$, the system gets back to $+m_0$ state and if $m_w < 0$, magnetization-reversal transition occurs and the system eventually chooses the $-m_0$ state (see figure 2). Thus setting $m_w = 0$, we obtain the threshold value of the pulse strength at the mean field phase boundary for this dynamic phase transition. At any T, combinations of h_p and Δt below the phase boundary cannot induce the magnetization-reversal transition, while those above it can induce the transition. From (8) therefore we can write the equation of the mean field phase boundary for the magnetization-reversal transition as

$$h_p^c(\Delta t, T) = \frac{\Delta T m_0}{1 - e^{-b\Delta T \Delta t}}. \tag{9}$$

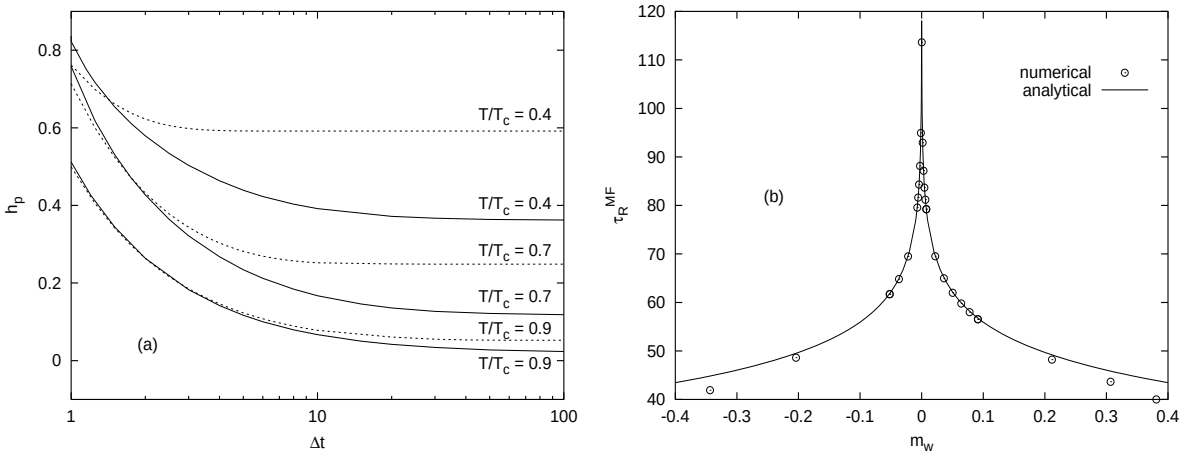

FIG. 3. (a) MF phase boundaries for three different temperatures. The solid line is obtained from numerical solution of (3) in MF case and the dotted lines give the corresponding analytical estimates in the linear limit (from [14]). (b) Logarithmic divergence of τ_R^{MF} across the phase boundary for $T/T_c = 0.9$. The data points (circles) for τ_R^{MF} are obtained from the solution of (4) (with $q = 0$, $|m(t) - m_w| < 10^{-4}$) and the solid line corresponds to (11) is the solution of the linearized MF equation (from [14]).

Figure 3a shows phase boundaries at different T obtained from (9) and compares those to the phase boundaries obtained from the numerical solution of the full dynamical equation (4). The phase boundaries obtained under linear approximation match quite well with those obtained numerically for small values of Δt and at temperatures close to T_c^{MF}, which is the domain of validity of the linearized theory as discussed before. In region III, we again have $h(t) = 0$ and solution of (5) leads to

$$m(t) = m_w \exp\left[b\Delta T\left\{t - (t_0 + \Delta t)\right\}\right]. \tag{10}$$

We define the relaxation time τ_R^{MF}, measured from $t = t_0 + \Delta t$, as the time required to reach the final equilibrium state characterized by magnetization $\pm m_0$ in region III (see figure 1). From above expression therefore we can write

$$\begin{aligned} \tau_R^{MF} &= \frac{1}{b\Delta T} \ln\left(\frac{m_0}{|m_w|}\right) \\ &\sim -\left(\frac{T}{T_c^{MF} - T}\right) \ln|m_w| \,. \end{aligned} \tag{11}$$

A point to note is that $m(t)$ in (10) grows exponentially with t and therefore in order to confine ourselves to the linear regime of $m(t)$, m_0 must be small (T close to T_c^{MF}) and $t \leq \tau_R^{MF}$. The factor $\left(T_c^{MF} - T\right)^{-1}$ gives the usual critical slowing down for the static transition at $T = T_c^{MF}$. However, even for $T \ll T_c^{MF}$, τ_R^{MF} diverges at the magnetization-reversal phase boundary where m_w vanishes. Figure 3b shows the divergence of τ_R^{MF} against m_w as obtained from the numerical solution of the full mean field equation of motion (4) and compares it with that obtained from (11).

Solution of $\chi_q(t)$ is more difficult as all the boundary conditions are not directly known. However, $\chi_q(t)$ can be expressed in terms of $m(t)$ and the solution of the resulting equation will then have the t dependence coming through $m(t)$, which we have solved already. Dividing (6) by (5) we get

$$\frac{d\chi_q(t)}{dm} = \frac{\chi_q(t) + \frac{1}{T(K(q)-1)}}{m(t)\left(\frac{K(0)-1}{K(q)-1}\right) + \frac{h(t)}{K(q)-1}}, \tag{12}$$

which can be rewritten in the linear limit as

$$\frac{d\chi_q}{\chi_q + \Gamma} = a_q \frac{dm}{m + h(t)/\Delta t}, \tag{13}$$

where $\Gamma = 1/T\left(K(q) - 1\right)$ and $a_q = \left(K(q) - 1\right) / \left(K(0) - 1\right) \simeq 1 - q^2/\Delta T$ for small q.

In region II, solution of (13) can be written as

$$\chi_q(t) = -\Gamma + \left(\chi_q^s + \Gamma\right)\left[\frac{m(t) - h_p/\Delta T}{m_0 - h_p/\Delta T}\right]^{a_q}, \tag{14}$$

where χ_q^s is the equilibrium value of susceptibility in region I. Solving (14) in region III with the initial boundary condition $m\left(t_0 + \Delta t\right) = m_w$, we get

$$\begin{aligned} \chi_q(t) &= -\Gamma + \left(\chi_q\left(t_0 + \Delta t\right) + \Gamma\right)\left(\frac{m(t)}{m_w}\right)^{a_q} \\ &= -\Gamma + \left(\chi_q^s + \Gamma\right)\left(\frac{m(t)}{m_w}\right)^{a_q} e^{b\Delta T \Delta t a_q}, \end{aligned} \tag{15}$$

where use has been made of (14) and (8). The dominating q dependence in $\chi_q(t)$ is coming from $(1/m_w)^{a_q}$ when $m_w \to 0$ as one approaches the phase boundary. The singular part of the dynamic susceptibility can then be written as

$$\chi_q(t) = \left(\chi_q^s + \Gamma\right) \exp\left[-q^2 \left(\xi^{MF}\right)^2\right], \tag{16}$$

where for small values of m_w the correlation length ξ^{MF} is given by [13, 14]

$$\xi^{MF} \equiv \xi^{MF}\left(m_w\right) = \left[\frac{T_c}{\Delta T} \ln\left(\frac{1}{|m_w|}\right)\right]^{\frac{1}{2}}. \tag{17}$$

Thus the length scale also diverges at the magnetization-reversal phase boundary and this can be demonstrated even using the linearized mean field equation of motion. Equations (11) and (17) can now be used to establish the following relation between the diverging time and length scales :

$$\tau_R^{MF} \sim \frac{T}{T_c} \left(\xi^{MF}\right)^2, \tag{18}$$

which leads to a dynamical critical exponent $z = 2$. One can have a numerical estimate of ξ^{MF} by solving (16) for different values of q. Figure 4(b) shows plots of $\chi_q(t)$ against m_w for different values of q. It may be noted that these divergences in τ_R^{MF} and ξ^{MF} are shown to occur for any $T < T_C^{MF}$, and these dynamic relaxation time and correlation length defined for the magnetization-reversal transition exist only for $T < T_c^{MF}$.

It may further be noted from (16) that $\chi_q(t) \to 0$ as $\xi^{MF} \to \infty$, thereby producing a minimum of χ_q at the phase boundary. The absence of any divergence in the susceptibility is due to the fact that at $t = t_0 + \Delta t$, there remains no contribution of m_w in $\chi_q(t)$ as is evident from (15). However, numerical solution of (12) for $q = 0$ mode shows a clear singularity in the homogeneous susceptibility χ_0 at the magnetization-reversal phase boundary ($m_w = 0$), as depicted in figure 4a.

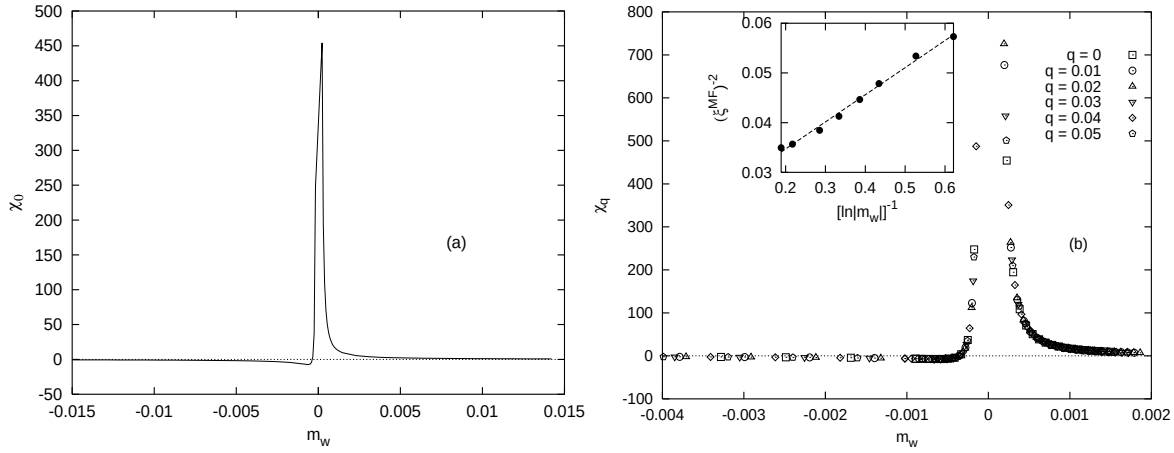

FIG. 4. (a) Divergence of $\chi_{q=0}$ across the phase boundary obtained from the numerical solution of (12). (b) Plot of χ_q against m_w for different values of q. The inset shows the linear variation of $\left(\xi^{MF}\right)^{-2}$ against $[\ln|m_w|]^{-1}$. The data points for ξ^{MF} in the inset are obtained from the slope of the best fitted straight lines through a plot of $\ln \chi_q$ against q^2 for different values of m_w (from [14]).

IV. MONTE-CARLO STUDY AND THE RESULTS

Here the Monte-Carlo study has been carried out in 2D and 3D (square and cubic lattices) with periodic boundary conditions. Spins are updated following Glauber dynamics. The updating rule employed here are both sequential as well as random. In sequential updating rule one Monte-Carlo step consist of a complete scan of the lattice in a sequential manner; while in random updating a Monte-Carlo step is defined by N $(= L^d)$ random updates on the lattice, where N is the total number of spins in a lattice of linear size L in d dimensions. Studies have been carried out at temperatures below the static critical temperature (e.g, $T_c^0 \simeq 2.27$ for 2D). The system is allowed to evolve from an initial state of perfect order to its equilibrium state at temperature T. The time t_0 is chosen to be much larger than the static relaxation time at that T, so that the system reaches an equilibrium state with magnetization $+m_0(T)$ before the external magnetic field is applied at time $t = t_0$. The field pulse of strength $-h_p$ is applied for duration Δt (measured in Monte Carlo steps or MCS). The magnetisation starts decreasing from its equilibrium value m_0. The average value of the magnetisation m_w at the time of withdrawal of pulse is noted. The phase boundary of this dynamic transition is defined by appropriate combination of h_p and Δt that produces the magnetisation reversal by making $m(t_0 + \Delta t) \equiv m_w = 0$ from a value $m(t_0) = m_0$, i.e, m_w changes sign across the phase boundary. The phase boundary changes with T. The behavior of different thermodynamic quantities are studied across the phase boundary. These quantities are averaged over different initial configurations of the system. The fluctuations over the average value are also noted.

We note the marked qualitative difference between the MF and MC phase boundaries (see Fig. 3 and Fig. 5). In the MF case, even for $\Delta t \to \infty$, due to absence of fluctuations, h_p must be greater than the non-zero coercive field in order that the transition takes place and the phase boundary becomes flat for large Δt. In MC study, due to presence

of fluctuations, even a pulse of infinitesimal strength, if applied for very long time, can induce the transition. This is evident from the asymptotic nature of the phase boundaries for large Δt.

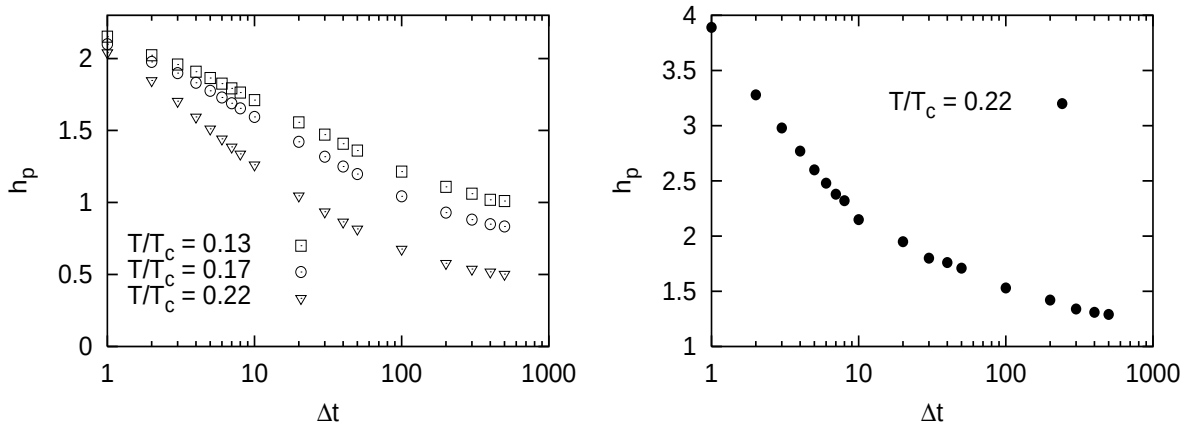

FIG. 5. Phase boundaries from Monte Carlo studies on square lattice with $L = 100$ for sequential updating (open symbols) [14] and random updating (filled symbol).

To understand the nature of the MC phase diagram of the magnetization-reversal transition we consult the classical theory of nucleation (CNT). A typical of a ferromagnet, below its static critical temperature T_c^0, consists of droplets or domains of spins oriented in the same direction, in a sea of oppositely oriented spins. According to CNT, the equilibrium number of droplets consisting of s spins is given by $n_s = N \exp(-\epsilon_s/T)$, where ϵ_s is the free energy of formation of a droplet containing s spins and N being the normalization constant. In presence of a negative external magnetic field h, the free energy can be written as $\epsilon_s = -2hs + \sigma s^{(d-1)/d}$, where the droplet is assumed to be spherical and $\sigma(T)$ is the temperature dependent surface tension. Droplets of size greater than a critical value s_c are favoured to grow, where $s_c = [\sigma(d-1)/(2d\,|h|)]^d$ is obtained by maximizing ϵ_s. The number of supercritical droplets is therefore given by $n_{s_c} = N \exp\left[-\Lambda_d \sigma^d\, |h|^{1-d}/T\right]$, where Λ_d is a constant depending on dimension only. In the SD regime, where a single supercritical droplet grows to eat up the whole system, the nucleation time goes inversely as the nucleation rate I. According to the Becker-Döring theory, I is proportional to n_{s_c} and therefore one can write

$$\tau_N^{SD} \propto I^{-1} \propto \exp\left[\frac{\Lambda_d \sigma^d}{T\,|h|^{d-1}}\right].$$

However, in the MD regime the nucleation mechanism is different and in this regime many supercritical droplets grow simultaneously and eventually coalesce to create a system spanning droplet. The radius $s_c^{1/d}$ of a supercritical droplet grows linearly with time t and thus $s_c \propto t^d$. For a steady rate of nucleation, the rate of change of magnetization is It^d. For a finite change Δm of the magnetization during the nucleation time τ_N^{MD}, one can write

$$\Delta m \propto \int_0^{\tau_N^{MD}} It^d dt = I\left(\tau_N^{MD}\right)^{d+1}.$$

Therefore, in the MD regime one can write [19][20]

$$\tau_N^{MD} \propto I^{-1/(d+1)} \propto \exp\left[\frac{\Lambda_d \sigma^d}{T(d+1)\,|h|^{d-1}}\right]. \tag{19}$$

During $t_0 \le t \le t_0 + \Delta t$, when the external field is 'on', the only relevant time scale in the system is the nucleation time. The magnetization reversal phase boundary gives the threshold value h_p^c of the pulse strength which, within time Δt, brings the system from an equilibrium state with magnetization $+m_0$ to a non-equilibrium state with magnetization $m_w = 0_-$, so that eventually the system evolves to the equilibrium state with magnetization $-m_0$. The field driven nucleation mechanism takes place for $t_0 \le t \le t_0 + \Delta t$ and therefore equating the above nucleation times with Δt, one gets for the magnetization-reversal phase boundary

$$\begin{aligned} \ln(\Delta t) &= c_1 + C\left[h_p^c\right]^{1-d}, && \text{in the SD regime} \\ &= c_2 + C\left[h_p^c\right]^{1-d}/(d+1), && \text{in the MD regime} \end{aligned} \tag{20}$$

where $C = \Lambda_d \sigma^d / T$ and c_1, c_2 are constants. Therefore a plot of $\ln(\Delta t)$ against $\left[h_p^c\right]^{d-1}$ would show two different slopes corresponding to the two regimes [15]. Figure 6 shows these plots and it indeed have two distinct slopes for both $d = 2$ (figure 6(a)) and $d = 3$ (figure 6(c)) at sufficiently high temperatures, where both the regimes are present. The ratio R of the slopes corresponding to the two regimes has got values close to 3 for $d = 2$ and close to 4 for $d = 3$, as suggested by (20). The value of h_{DSP} is obtained from the point of intersection of the straight lines fitted to the two regimes. At lower temperatures, however, the MD region is absent and the phase diagram here is marked by a single slope as shown in figures 6(b) and 6(d).

The relaxation behaviour follows :

$$\tau_R \sim \kappa(T, L) e^{-\mu(T)|m_w|}, \tag{21}$$

where $\kappa(T, L)$ is a constant depending on temperature and system size and $\mu(T)$ is a constant depending on temperature only. It may be noted from (21) that $\tau \to \kappa(T, L)$ as $m_w \to 0$. Therefore the true divergence at the phase boundary (where $m_w = 0$) of the relaxation time depends on the nature of $\kappa(T, L)$. $\kappa(T, L)$ grows sharply with system size. The relaxation time τ_R therefore diverges in the thermodynamic limit ($L \to \infty$) through the constant κ. It may be noted that this divergence of τ_R at the dynamic magnetization-reversal phase boundary occurs even at temperatures far below the static critical temperature T_c^0.

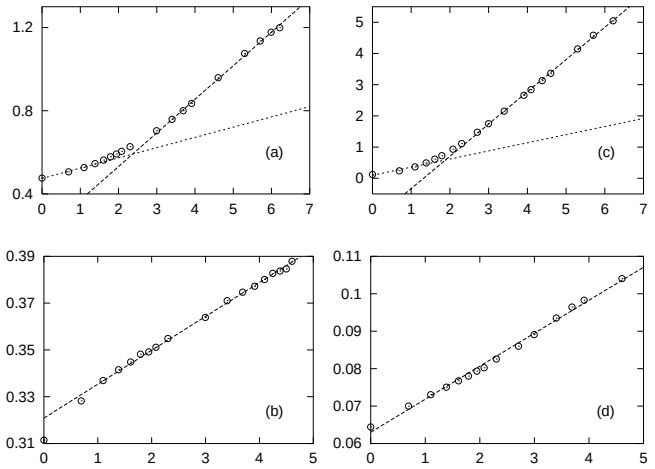

FIG. 6. Plots of $\ln \Delta t$ against $(h_p)^{1-d}$ along the MC phase boundary. (a) $T/T_c = 0.31$ and (b) $T/T_c = 0.09$ for square lattice and (c) $T/T_c = 0.67$ and (d) $T/T_c = 0.11$ for simple cubic lattice. The slope ratio $R \simeq 3.27$ in (a) and $\simeq 3.97$ in (c) (from [14]).

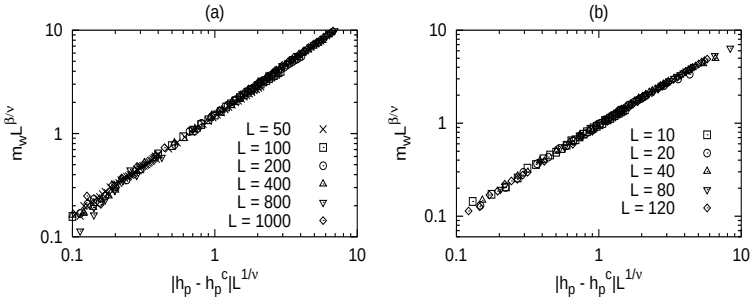

FIG. 7. Finite size scaling fits : (a) for $d = 2$ at $T/T_c = 0.88$ and (b) for $d = 3$ at $T/T_c = 0.67$ (from [14]).

In the region where the transition is continuous, the scaling arguements are expected to hold. We assume power law behaviour in this regime both for m_w

$$m_w \sim \left| h_p - h_p^c \left(\Delta t, T \right) \right|^{\beta} \tag{22}$$

and for the correlation length

$$\xi \sim \left| h_p - h_p^c \left(\Delta t, T \right) \right|^{-\nu}. \tag{23}$$

For a finite size system, h_p^c is a function of the system size L. Assuming that at the phase boundary ξ can at the most reach a value equal to L, one can write the finite size scaling form of m_w as:

$$m_w \sim L^{-\beta/\nu} f\left[\left(h_p - h_p^c\left(\Delta t, T, L\right)\right) L^{1/\nu}\right], \tag{24}$$

where $f(x) \sim x^{\beta/\nu}$ as $x \to \infty$. A plot of $m_w/L^{-\beta/\nu}$ against $\left(h_p - h_p^c\left(\Delta t, T, L\right)\right) L^{1/\nu}$ shows a nice collapse of the data for $d = 2$ and for $d = 3$ as shown in figure 7. The values of the critical exponents obtained from the data collapse were $\beta = 0.85 \pm 0.05$ and $\nu = 1.5 \pm 0.5$ in $d = 3$ and $\beta = 1.00 \pm 0.05$ and $\nu = 2.0 \pm 0.5$ in $d = 2$, where $h_p^c\left(\Delta t, T\right)$ was obtained with an accuracy $O\left(10^{-3}\right)$. Attempts to fit similar data to the above finite size scaling form obtained in the SD regime failed.

The behavior of the reduced fourth order cumulant U [21] has also been studied near the magnetisation reversal transition boundary. This is defined as

$$U = 1 - \frac{\left\langle m_w^4 \right\rangle}{3\left\langle m_w^2 \right\rangle^2}, \tag{25}$$

where $\left\langle m_w^4 \right\rangle$ is the ensemble average of m_w^4. $\left\langle m_w^2 \right\rangle$ is similarly defined. The cumulant U here behaves somewhat differently, compared to that in static and other transitions: Deep inside the ordered phase $m_w \simeq 1$ and $U \to 2/3$. For other (say, static) transitions the order parameter (m_w) goes to zero with a Gaussian fluctuation above the transition point, giving $U \to 0$ there. Here, however, due to the presence of the pulsed field, $|m_w|$ is non-zero on both sides of the magnetisation-reversal transition. Hence U drops to zero at a point near the transition and grows again after it.

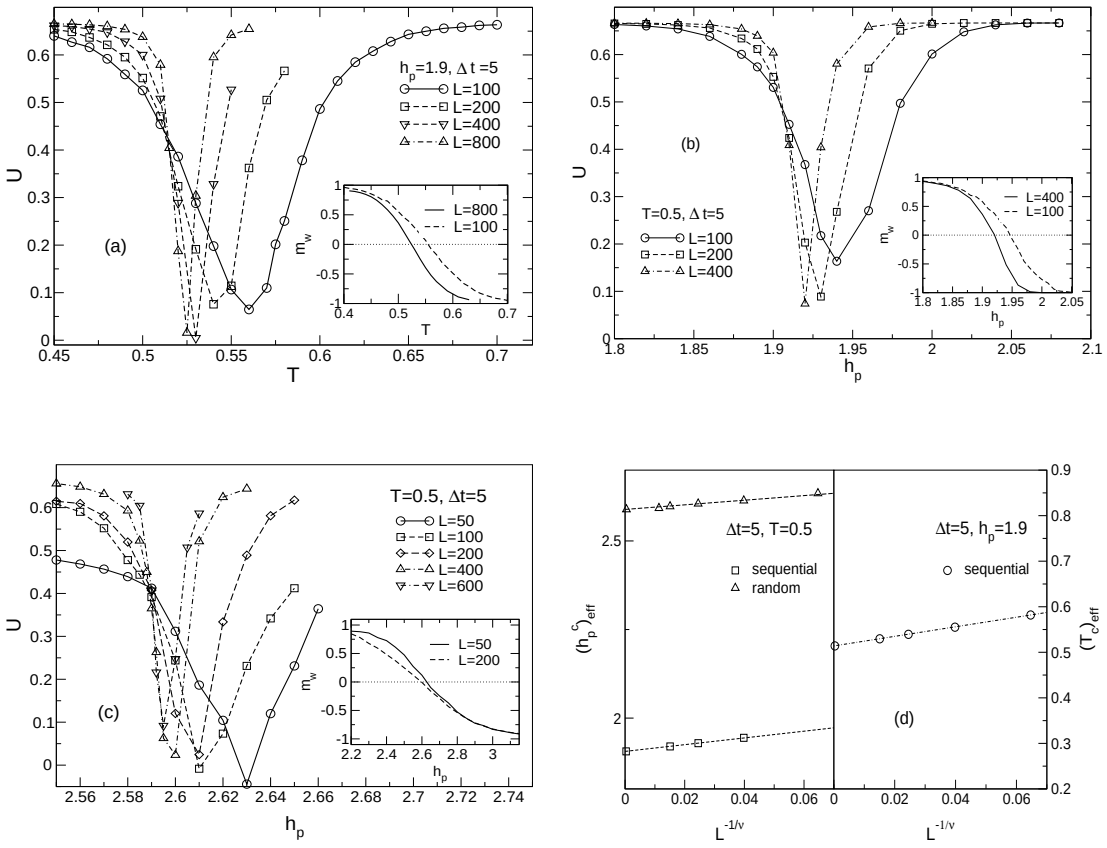

FIG. 8. Behavior of U near the transition, driven by (a) T at a fixed value of h_p (=1.9) and Δt (=5) with sequential updating, (b) h_p at a fixed value of T (=0.5) and Δt (=5) with sequential updating, and (c) h_p at a fixed value of T (=0.5) and Δt (=5) with random updating, for different L, averaged over 1000 to 20000 initial configurations. The insets show the typical behavior of the magnetisation m_w at the time of withdrawal of the field pulse by varying (a) T at a fixed h_p and Δt, for $L = 100$ and 800, (b) h_p at a fixed T and Δt, for $L = 100$ and 400, (c) h_p at a fixed T and Δt, for $L = 50$ and 200; $m_w = 0$ at the effective transition point. (d) Finite size scaling

study in this parameter range: the effective T_c or h_p^c values (see the insets), where $m_w = 0$, are plotted against $L^{-1/\nu}$ with $\nu^{-1} = 0.7$. The values of the cumulant crossing points in (a), (b), (c) are taken to correspond the respective transition points for $L \to \infty$ (from [7]).

The universality class of the dynamic transition in Ising model under oscillating field has been studied extensively by investigating [5] the critical point and the cumulant value U^* at the critical point, where the cumulant curves cross for different system sizes (L). In that case, of course, the variation of U (at any fixed L) is similar to that in the static Ising transitions ($U = 2/3$ well inside the ordered phase and $U \to 0$ well within the disordered phase). In fact, U^* value in this oscillatory field case was found to be the same as that in the static case, indicating the same universality class [5]. We have studied the behavior of U in 2D. We observe different behavior in the field pulse induced magnetisation-reversal transition case.

We observed [7] two distinct behavior of the cumulant U. Typically, for low temperature and low pulse-duration region (see the inset in Fig. 2) of the magnetisation-reversal phase boundary, the cumulant crossing for different system sizes (L) occur at $U^* \simeq 0.42$ to 0.46 (see Fig. 8). We checked these results for both sequential and random updating. Specifically, for $T = 0.5$ and $\Delta t = 5$, (see Fig. 8c) for random updating we find the transition point value of $h_p \simeq 2.6$, to be smaller than the value ($\simeq 1.9$) for sequential updating. However, the value of U^* at this transition point is very close to about 0.44. This indicates that updating rule does not affect the universality class (U^* value), as long as the proper region of the phase boundary is considered. For relatively higher temperature and pulse-duration region of the phase boundary, the crossing of U for different L values occur for $U^* \simeq 0_+$. This occurs both for sequential (Fig. 9a, b) and random (Fig. 9c) updating. It may be noted that the phase boundary changes with the updating rule, as the system relaxation time (which matches with the pulse width at the phase boundary) is different for sequential and random updating [21].

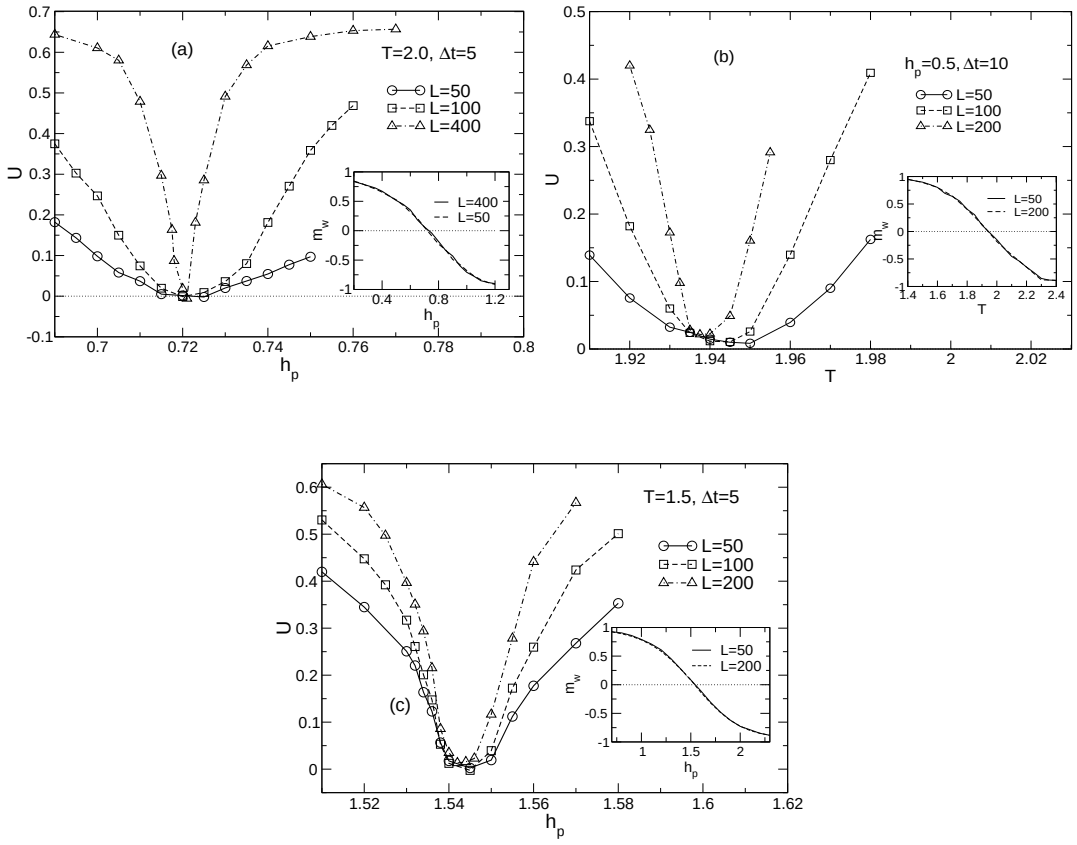

FIG. 9. Behavior of U near the transition, driven by (a) h_p at a fixed value of T (=2.0) and Δt (=5) with sequential updating, (b) T at a fixed value of h_p (=0.5) and Δt (=10) with sequential updating, and (c) h_p at a fixed value of T (=1.5) and Δt (=5) with random updating, for different L, averaged over 1000 to 6000 initial configurations. The insets show the typical behavior of the magnetisation m_w at the time of withdrawal of the field pulse by varying (a) h_p at a fixed T and Δt, for $L = 50$ and 400, (b) T at a fixed h_p and Δt, for $L = 50$ and 200, (c) h_p at a fixed T and Δt, for $L = 50$ and 200; $m_w = 0$ at the transition point (from [7]).

Note that in the low temperature and Δt regions, there seems to be significant finite size scaling of the transition ($m_w = 0$) point (see the insets of Fig. 8a, b, c). In Fig. 8d, the finite-size scaling analysis of those data is presented. For the other cases, there seems to be no significant finite size effect on the transition point (cf. insets of Fig. 9a, b,

c), indicative of a mean-field nature of the transition in this range. It may be noted that to compare the finite size effects, we normalise the parameters T or h_p by their ranges required for full magnetisation reversal. In fact, this weak finite size effect for high T and Δt regions did not lead to any reasonable value for the fitting exponent in the scaling analysis.

For the static transition of the pure two-dimensional Ising system, $U^* \simeq 0.6107$ [21, 22]. For low temperature (and low Δt) regions of the magnetisation-reversal phase boundary, the observed values of U^* (in the range 0.42 - 0.46) are considerably lower than the above mentioned value for the static transition. There is not enough indication of finite-size effect in the U^* value either (cf. [5]). This suggests a new universality class in this range. Also, the finite-size scaling study for the effective transition points here (see Fig. 8d) gives a correlation length exponent value ($\nu \simeq 1.4$) [7] larger than that of the static transition. This value of the exponent ν compares well with that obtained by the data collapse ($\nu = 2.0 \pm 0.5$ in $d = 2$) [14]. For comparatively higher temperatures (and high Δt), the $U^* \simeq 0_+$ at the crossing point. Such small value of the cumulant at the crossing point can hardly be imagined to be a finite-size effect; it seems unlikely that one would get here also the same universality class and U^* value will eventually shoot up to $U^* \simeq 0.44$ (for larger system sizes), as for the other range of the transition. On the other hand, such low value of U^* might indicate a very weak singularity, as indicated by the mean field calculations [13] mentioned in the introduction. In fact, even for the static transition, as the dimensionality increases, and the singularity becomes weaker (converging to mean field exponents) with increasing lattice dimension, the cumulant crossing point U^* decreases ($U^* \simeq 0.61$ in $d = 2$ to $U^* \simeq 0.44$ in $d = 4$). We believe the mean field transition behavior here, as mentioned earlier, is even weaker in this dynamic case as reflected by the value $U^* \simeq 0_+$, corresponding to a logarithmic singularity (as in eqns. (11) and (17)).

V. SUMMARY AND CONCLUSIONS

In this paper, we review all the aspects studied so far on the dynamic magnetization-reversal phenomena in the Ising model under a finite-duration external magnetic field competing with the existing order for $T < T_c^0$. We have discussed the mean-field equation of motion and its solution, the nature of the MF phase boundary and the divergence of the susceptibility and relaxation time. The analytic solution of the linearized equation of motion also showed divergence of susceptibility and relaxation time on the MF phase boundary [13]. The same transition has been studied by Monte Carlo simulations in both two and three dimensions. The obtained phase diagram is consistent with the classical nucleation theory. The nucleation process is initiated by the external magnetic field and depending on the strength of the field the system nucleates either through the growth of a single droplet or through the growth and subsequent coalescence of many droplets. For $h_p > h_{DSP}$ the system belongs to the multi-droplet regime and the transition is continuous in nature; whereas for $h_p < h_{DSP}$ the system goes over to the single-droplet regime where transition is discontinuous. Expecting power law behaviour for both m_w and ξ in multi-droplet regime, the finite size scaling fits give the estimates of the critical exponents β and ν for both $d = 2$ and 3. Unlike in the MF case, where the relaxation time τ_R^{MF} shows a logarithmic divergence, τ_R in MC studies falls off exponentially away from $m_w = 0$ and the divergence in τ_R comes through the growth of the prefactor κ with the system size.

The universality class of the dynamic magnetisation-reversal transition in 2D, has been studied here using Monte Carlo simulations. Both sequential and random updating have been used. The phase boundary at any T ($< T_c^0$) is obtained first in the $h_p - \Delta t$ plane. They of course depend on the updating rule. The phase boundaries obtained compare well with the nucleation theory estimate $h_p \ln \Delta t$ = constant along the boundary [11, 16]. Extensive Monte-Carlo studies for the fluctuations in the order parameter $|m_w|$ and internal energies etc. showed prominent divergences along the phase boundaries [6]. Fourth order cumulant (U) of the order parameter distribution is also studied for different system sizes (upto $L = 800$) around the phase boundary region [7]. The crossing point of the cumulant (for different system sizes) gives the transition point and the value U^* of the cumulant at the transition point indicates the universality class of the transition. In the low temperature and low pulse width range, the U^* value is found to be around 0.44 [7] (see Figs. 8a, b, c). The prominent discripancy with the U^* value ($\simeq 0.61$) for the static transition in the same model in two dimensions indicates a new universality class for this dynamic transition. Indeed, the finite-size scaling analysis (Fig. 8d) suggests a different (larger) value of the correlation length exponent also. For comparatively higher temperatures and higher pulse widths, the U^* values are very close to zero (see Fig. 9a, b, c), and the transitions here seem to fall in a mean-field-like weak-singularity universality class similar to that obtained earlier [13], and indicated by eqns. (11) and (17). Here, the finite size effects in the order parameter and the transition point are also observed to be comparatively weaker (see insets of Fig. 9).

Acknowledgments

The authors are grateful to Arkajyoti Misra for some useful discussions.

---

[1] Y. Martin and H. Wickramsinghe, Appl. Phys. Lett. **50** (1987) 1455; M. Lederman, S. Schultz, M. Ozaki, Phys. Rev. Lett. **73** (1994) 1986.
[2] D. Sander, A. Enders, R. Skomski and J. Kirschner, IEEE Trans. Magn. **32** (1996) 4570; H. J. Elmers, J. Hauschild, H. Fritzsche, G. Liu, U. Gradmann and U. Köhler, Phys. Rev. Lett. **75** (1995) 2031.
[3] H. J. Elmers, J. Hauschild, H. Höche, U. Gradmann, H. Bethge, D. Heuer and U. Köhler, Phys. Rev. Lett. **73** (1994) 898.
[4] B. K. Chakrabarti and M. Acharyya, Rev. Mod. Phys. **71** (1999) 847.
[5] G. Korniss, P. A. Rikvold and M. A. Novotny, Phys. Rev. E **66** (2002) 056127; K. Park et al, Phys. Rev. Lett. **92** (2004) 015701.
[6] B. K. Chakrabarti and A. Misra, Comp. Phys. Comm. **147** (2002) 120, *cond-mat/0109188*.
[7] A. Chatterjee and B. K. Chakrabarti, Phys. Rev. E. **67** (2003) 046113.
[8] T. Tóme and M. J. de Oliveira, Phys. Rev. A **41** (1990) 4251.
[9] M. Acharyya and B. K. Chakrabarti, Phys. Rev B **52** (1995) 6550;
[10] I. Junier and J. Kurchan, Europhys. Lett. **63** (2003) 674.
[11] M. Acharyya, J. K. Bhattacharjee and B. K. Chakrabarti, Phys. Rev. E **55** (1997) 2392.
[12] A. Misra and B. K. Chakrabarti, Physica A **246** (1997) 510; Phys. Rev. E **58** (1998) 4277.
[13] R. B. Stinchcombe, A. Misra and B. K. Chakrabarti, Phys. Rev. E **59** (1999) R4717.
[14] A. Misra and B. K. Chakrabarti, J. Phys. A **33** (2000) 4249.
[15] A. Misra and B. K. Chakrabarti, Europhys. Lett. **52** (2000) 311.
[16] A. Misra, *Non-equilibrium Transitions in Classical Spin Systems*, Ph.D Thesis, Jadavpur Univ. (2000).
[17] V. G. Voznyuk, A. Misra, W. D. Doyle and P. B. Visscher, available at: http://bama.ua.edu/∼arko/CP-15.pdf.
[18] M. Suzuki and R. Kubo, J. Phys. Soc. Japan **24** (1968) 51.
[19] P. A. Rikvold, H. Tomita, S. Miyashita and S. W. Sides, Phys. Rev. E **49** (1994) 5080.
[20] M. Acharyya and D. Stauffer, Euro. Phys. J. B **5** (1998) 571.
[21] K. Binder and D. Heermann, *Monte Carlo Simulation in Statistical Physics*, (Springer, Berlin, 1988).
[22] G. Kamieniarz and H. Blöte, J. Phys. A **26** (1993) 201.